

Seabed morphology and bed shear stress predict temperate reef habitats in a high energy marine region

Jackson-Bue, Tim; Williams, Gareth; Whitton, Timothy; Roberts, Michael; Goward Brown, Alice; Amir, Hana; King, Jonathan; Powell, Ben; Rowlands, Steven; Llewelyn Jones, Gerallt; Davies, Andrew

Estuarine, Coastal and Shelf Science

DOI:

<https://doi.org/10.1016/j.ecss.2022.107934>

Published: 05/09/2022

Peer reviewed version

[Cyswllt i'r cyhoeddiad / Link to publication](#)

Dyfyniad o'r fersiwn a gyhoeddwyd / Citation for published version (APA):

Jackson-Bue, T., Williams, G., Whitton, T., Roberts, M., Goward Brown, A., Amir, H., King, J., Powell, B., Rowlands, S., Llewelyn Jones, G., & Davies, A. (2022). Seabed morphology and bed shear stress predict temperate reef habitats in a high energy marine region. *Estuarine, Coastal and Shelf Science*, 274, Article 107934. <https://doi.org/10.1016/j.ecss.2022.107934>

Hawliau Cyffredinol / General rights

Copyright and moral rights for the publications made accessible in the public portal are retained by the authors and/or other copyright owners and it is a condition of accessing publications that users recognise and abide by the legal requirements associated with these rights.

- Users may download and print one copy of any publication from the public portal for the purpose of private study or research.
- You may not further distribute the material or use it for any profit-making activity or commercial gain
- You may freely distribute the URL identifying the publication in the public portal ?

Take down policy

If you believe that this document breaches copyright please contact us providing details, and we will remove access to the work immediately and investigate your claim.

Seabed morphology and bed shear stress predict temperate reef habitats in a high energy marine region

Tim Jackson-Bu  ^{*1,2}, Gareth J. Williams², Timothy A. Whitton^{1,2}, Michael J. Roberts^{1,2}, Alice Goward Brown^{1,2}, Hana Amir², Jonathan King^{1,2}, Ben Powell², Steven J. Rowlands^{1,2}, Gerallt Llewelyn Jones³ & Andrew J. Davies⁴

* Corresponding author. Email: t.d.jackson@bangor.ac.uk

¹ Centre for Applied Marine Sciences, Bangor University, Askew St, Menai Bridge, LL59 5AB, UK

² School of Ocean Sciences, Bangor University, Askew St, Menai Bridge, LL59 5AB, UK

³ Menter Môn Cyf, Neuadd Y Dref Llangefni, Sgwar Bulkeley, Llangefni, Ynys Môn LL77 7LR

⁴ University of Rhode Island, Center for Biotechnology and Life Sciences, 120 Flagg Road, Kingston, RI 02881, USA

ORCID IDs:

TJB: 0000-0001-7077-2186

GJW: 0000-0001-7837-1619

TAW: 0000-0002-8043-9229

MJR:

AGB: 0000-0002-9089-6861

HA: 0000-0001-9625-6294

JK: 0000-0002-4106-9368

BP: 0000-0003-4358-7289

SJR: 0000-0002-7969-3705

GLJ:

AJD: 0000-0002-2087-0885

Abstract

High energy marine regions host ecologically important habitats like temperate reefs, but are less anthropogenically developed and understudied compared to lower energy waters. In the marine environment direct habitat observation is limited to small spatial scales, and high energy waters present additional logistical challenges and constraints. Semi-automated predictive habitat mapping is a cost-effective tool to map benthic habitats across large extents, but performance is context specific. High resolution environmental data used for predictive mapping are often limited to bathymetry, acoustic backscatter and their derivatives. However, hydrodynamic energy at the seabed is a critical habitat structuring factor and likely an important, yet rarely incorporated, predictor of habitat composition and spatial patterning. Here, we used a machine learning classification approach to map temperate reef substrate and biogenic reef habitat in a tidal energy development area, incorporating bathymetric derivatives at multiple scales and simulated tidally induced seabed shear stress. We mapped reef substrate (four classes: sediment (not reef), stony reef (low resemblance), stony reef (medium – high resemblance) and bedrock reef) with overall balanced accuracy of 71.7%. Our model to predict potential biogenic *Sabellaria spinulosa* reef performed less well with an overall balanced accuracy of 63.4%. Despite low performance metrics for the target class of potential reef in this model, it still provided insight into the importance of different environmental variables for mapping *S. spinulosa* biogenic reef habitat. Tidally induced mean bed shear stress was one of the most important predictor variables for both reef substrate and biogenic reef models, with ruggedness calculated at multiple scales from 3 m to 140 m also important for the reef substrate model. We identified previously unresolved relationships between temperate reef spatial distribution, hydrodynamic energy and seabed three-dimensional structure in energetic waters. Our findings contribute to a better understanding of the spatial ecology of high energy marine ecosystems and will inform evidence-based decision making for sustainable development, particularly within the growing tidal energy sector.

Keywords

Reef mapping, bathymetry, tidal energy, machine learning, seascape ecology, spatial scale, *Sabellaria spinulosa*, benthic ecology, hydrodynamics, ecosystem management.

1. Introduction

To understand ecological pattern and process, reliable information about the spatial distribution of habitats is essential (Brown et al., 2011; Cogan et al., 2009; Turner, 1989). Aerial and satellite remote sensing has revolutionised spatial ecology, providing spatially continuous data on a variety of ecologically relevant variables at high resolution across broad extents (Kerr and Ostrovsky, 2003; McDermid et al., 2005). This type of information is more challenging to collect for the seabed beyond the shallow clear waters that can be observed with optical remote sensing (D'Urban Jackson et al., 2020; Lecours et al., 2015). Advances in acoustic remote sensing now enable collection of high-resolution ($< 1\text{m}$), spatially continuous seabed bathymetry and acoustic reflectivity (commonly referred to as backscatter). However, detailed seabed mapping is still costly and inefficient compared to terrestrial remote sensing, such that less than 18% of the oceans has depth measurements at 1 km resolution or better (Mayer et al., 2018). Other seabed properties, including benthic habitat characteristics, are even more challenging to map. Methods for observing seafloor habitats and organismal communities are limited to fine to moderate spatial scales (0.01 m – 1 km) using diver, camera, crewed/uncrewed vehicle, acoustic or physical sampling (van Rein et al., 2009). To generate spatially continuous benthic habitat maps over large extents, practitioners use statistical approaches to identify relationships between discrete habitat observations and spatially continuous environmental data and extrapolate into unobserved locations (Brown et al., 2011).

Temperate reefs are hard-bottom marine habitats between the tropics and the poles, and include biodiverse ecosystems that provide billions of dollars in ecosystem goods and services (Bennett et al., 2016; Taylor, 1998). Temperate reef substrate may be bedrock or stony (geogenic) or derived from organisms (biogenic), both hosting communities of sessile and mobile reef-associated species (Bué et al., 2020; Diesing et al., 2009; Holbrook et al., 1990). Due to their ecological importance reef habitats are listed in various national and international conservation legislation, including Annex 1 of the European Commission Habitats Directive (European Commission, 2013). However, a lack of information about the distribution and characteristics of reef habitats hampers effective ecosystem management (Diesing et al., 2009). Temperate reef habitats are often found in high energy marine waters (Warwick and Uncles, 1980). These areas are challenging and costly to operate within compared to lower energy seas and as such they are less anthropogenically developed and less well studied (Shields et al., 2011). In response to the global demand for low carbon energy, energetic waters are now of commercial interest to the nascent marine renewable energy industry (Roche et al., 2016). To ensure sustainable development, there is a growing need for baseline ecosystem information about energetic waters. While previous attempts at mapping temperate reefs have shown some

success, it has proved challenging to distinguish between specific reef types like bedrock and stony reef, and between reef and non-reef ground without considerable manual input (Dalkin, 2008; Eggleton and Meadows, 2013; Limpenny et al., 2010; Plets et al., 2012; Vanstaen and Eggleton, 2011). Biogenic temperate reefs are similarly challenging to map, typically requiring manual interpretation and digitisation of acoustic information (Jenkins et al., 2018; Limpenny et al., 2010; Lindenbaum et al., 2008; Pearce et al., 2014). There is a growing need for repeatable, cost-effective habitat mapping in high energy waters, to understand the spatial ecology of these understudied ecosystems and to support sustainable management in an evolving seascape of offshore activity (Dannheim et al., 2020; Jouffray et al., 2020; Wilding et al., 2017).

Bathymetry, backscatter intensity and their derivatives are typically the main, or only environmental predictor variables in benthic habitat models beyond shallow, clear waters, as few other variables can be recorded at a comparable resolution. However, numerous other variables are important in structuring benthic habitats. For example, water chemistry and temperature, when modelled at appropriate spatial scales, can be important predictors of benthic habitats (Davies and Guinotte, 2011). Hydrodynamic energy at the seabed is an important structuring factor for benthic habitats and communities. As well as imparting mechanical stress (Gove et al., 2015; Koehl, 1999), water flow controls water chemistry (Gutiérrez et al., 2008), particulate food supply (Rosenberg, 1995; Sebens et al., 1998) and larval dispersal (Cowen and Sponaugle, 2009). Alteration of flow regimes affects feeding efficiency, growth rates and settlement of benthic species that are adapted to specific flow conditions (Eckman and Duggins, 1993). Critically, hydrodynamic energy affects substrate composition through sediment transport (Shields, 1936), which in turn controls benthic community composition and imparts temporal variation within the system (Coggan et al., 2012; Warwick and Uncles, 1980). Hydrodynamic energy has proved to be an important variable for mapping benthic habitat spatial distribution at regional and national scales with resolution of kilometres (Huang et al., 2011; Robinson et al., 2011), but it is often overlooked or unavailable for predictive mapping at finer scales (Brown et al., 2011; Pearman et al., 2020). The inclusion of simulated wave induced seabed energy improved predictive habitat mapping for a wave exposed region in temperate southern Australia (Rattray et al., 2015), and it follows that tidally induced seabed energy is likely to be an important predictor of high energy habitats in regions with fast tidal currents. However, to our knowledge no study has incorporated tidally induced energy at the seabed with high-resolution bathymetry for predictive habitat mapping in temperate, high tidal energy waters.

Tidally induced hydrodynamic energy is likely to influence the distribution of geogenic and biogenic reefs in different ways. Strong tidal currents erode and transport sediment, leaving

stable substrates that may be colonised by epibiota to form geogenic reefs. For biogenic reefs, the effects of hydrodynamic energy depend on the reef-forming organism. *Sabellaria spinulosa* is a reef-forming annelid that builds aggregations of tubes from suspended coarse sediment, supporting diverse associated communities (Pearce, 2017). *S. spinulosa* reef distribution is likely to be influenced by the availability of resuspended sediment as tube-building material, in turn driven by hydrodynamic energy (Davies et al., 2009; Holt et al., 1998). We used semi-automated predictive mapping, parameterized with multibeam echo sounder derived variables and incorporating simulated hydrodynamic energy data, to map previously unresolved potential reef habitats in a marine area of interest for tidal energy development. We show that tidally induced bed shear stress is a highly important variable for predicting high energy reef habitats. Our findings provide a deeper understanding of the relationships between hydrodynamic conditions, seabed morphology and reef habitats, with implications for sustainable development of understudied, high tidal energy waters.

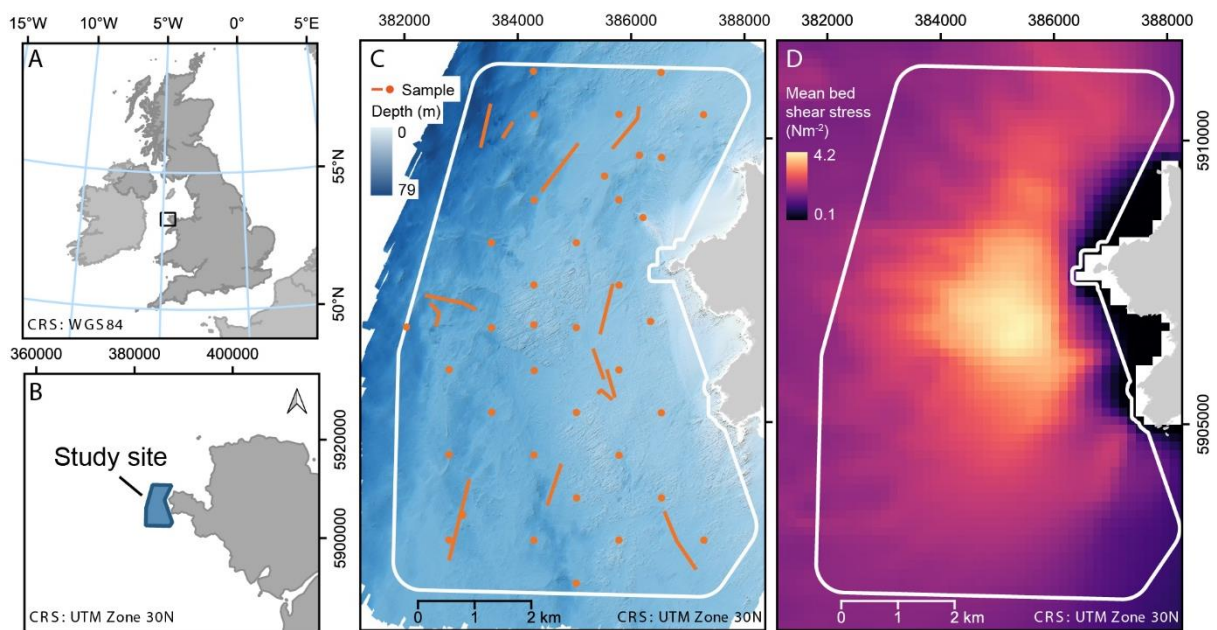


Figure 1. A & B) Location of the study site (black square in A) in north west Wales, UK. C) Bathymetry of the study area (white boundary) showing point and transect drop-down video sampling locations. D) Modelled tidally induced mean bed shear stress across the study area.

2. Method

2.1 Study Site

We mapped potential reef habitats in a 49 km² area to the west of Sir Ynys Môn (Isle of Anglesey), Wales, UK (Fig. 1). Our study area comprised a 500 m buffer around a 35 km² area leased for tidal energy device demonstration, which was then buffered inwards by 100 m from the edge of input data extent to avoid edge effects. Tidal current speeds at the site reach 3.7 m s⁻¹ and annual mean significant wave height is 1.26 to 1.5 m (Royal Haskoning DHV, 2019). Water depth within the study area ranges from 3-79 m (Fig. 1C) and the seabed comprises a range of benthic habitats from mobile sediment to stable cobble and bedrock colonised by slow growing epifauna (Whitton, 2014). The site is known to contain potential reef, but the spatial distribution of different reef types in the area is unresolved (MarineSpace, 2019).

2.2 Habitat Observations





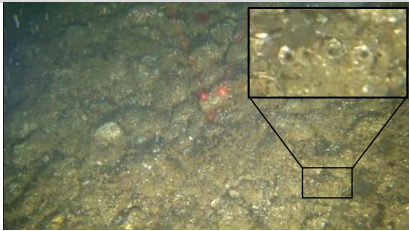
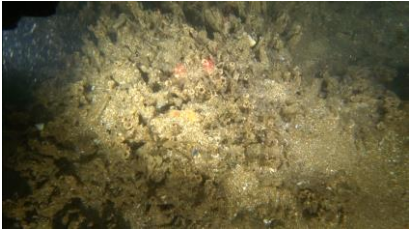
We collected seabed video samples within the study site in June and July 2019 using the RV Prince Madog (Fig. 1C, transect samples), with further samples obtained from a commercial ecological survey of the study site (Fig. 1C, point samples). Sampling locations were spatially well-distributed, captured a range of energy conditions, and targeted areas of the study site with visually different bathymetric features. For transect video samples we used high-resolution video (1080p, 60 frames per second) with a forward facing (45° to the seabed), mechanically stabilised camera (FDR X3000, Sony), with dive lights for illumination and parallel lasers for scaling. To record sampling positions, we used an ultra-short baseline (USBL) system (EasyTrak Nexus Lite, Applied Acoustics) calibrated to a horizontal accuracy of 8 m. We sampled transects by drifting for 1 hour or 1 km within an hour either side of slack water, in current speeds of less than 1 kt.

To extract discrete observation data without introducing multiple operator errors, a single operator reviewed and classified the transect video footage. Starting from 1 min after the frame started moving steadily on the seabed, we assigned a class for reef substrate and a class for potential *S. spinulosa* reef (Table 1) to each 30 s section. Classes were derived from published definitions of reef habitat categories developed to aid environmental management, conservation and spatial planning, in which benthic habitats are categorised according to how closely they resemble stony reef or biogenic *Sabellaria spinulosa* reef (Hendrick and Foster-Smith, 2006; Irving, 2009; Limpenny et al., 2010). We only recorded observations for sections in which the seabed was visible at close enough range to confidently assess particle size using the parallel lasers for at least 50% of the section. We classified reef substrate as sediment (not reef), stony

reef (low resemblance), stony reef (mid-high resemblance) or bedrock (Irving, 2009). While we initially classified stony reef into three resemblance classes, there were few high resemblance observations, so we combined mid and high resemblance observations (Table 1). We classified potential biogenic (*Sabellaria spinulosa*) reef separately to substrate because *S. spinulosa* can colonise a range of substrates, and initial data exploration indicated that the predictor variables we used, mainly morphological descriptors, were unlikely to distinguish between stony reef and stony reef colonised by *S. spinulosa*. After preliminary data exploration we classified *S. spinulosa* observations as not reef, comprising samples with no *S. spinulosa* tubes present and those with individual tubes of less than 10% cover, and potential reef, comprising samples with colonies over 2 cm high or more than 10% cover (Table 1). We extracted positions of the video observations to within 8 m horizontal accuracy by matching the video timestamps to the USBL timestamps. Data from one transect were discarded due to low positional accuracy.

We reclassified an additional point video sample dataset obtained from a commercial ecological survey of the study site to our classification system based on the percent cover of substrates and *S. spinulosa* reef recorded. These data were derived from drop down video sampling of the study area in 2018 and had been analysed for biotope mapping with percent cover of species and substrates quantified (MarineSpace, 2019). We gridded the combined transect and point video observations on a 20 m resolution grid matching the environmental data, assigning the class with the highest rank (Table 1) where there were multiple observations in a grid cell to give a single observation per grid cell. We had total of 500 and 509 observations for substrate and *Sabellaria spinulosa* respectively, the difference due to *S. spinulosa* reef obscuring the substrate in some samples.

Table 1. Drop-down video classification. Each 30 second section of video was assigned a class for reef substrate and potential biogenic reef. Class ranks were used to reduce multiple observations to a single ground truth observation per pixel of environmental data. Distance between laser points = 50 mm.

CLASS	QUALIFIER	RANK	EXAMPLE
REEF SUBSTRATE			
SEDIMENT (NOT REEF)	Less than 10% particles of 64 mm or more.	1	
STONY REEF (LOW RESEMBLANCE)	10 – 40% particles of 64 mm or more. Epifauna present.	2	
STONY REEF (MID-HIGH RESEMBLANCE)	Over 40 % particles of 64 mm or more. Epifauna present.	3	
BEDROCK REEF	Bedrock present	4	
BIOGENIC REEF			
NOT <i>S. SPINULOSA</i> REEF	No <i>S. spinulosa</i> tubes seen, or <i>S. spinulosa</i> tubes present but covering less than 10%	1	
POTENTIAL <i>S. SPINULOSA</i> REEF	<i>S. spinulosa</i> colonies of over 2 cm height or with over 10% cover	2	

2.3 Environmental predictor variables

To predict the spatial distribution of potential reef habitats we used morphological derivatives from bathymetry data and a measure of seabed energy as environmental predictor variables (Table 2). Bathymetry data (1 m horizontal resolution) were collected using a multibeam echosounder (MBES) for the study site in 2018 during a commercial survey (Royal Haskoning DHV, 2019) (Fig. 1C). We generated six morphological derivatives from the bathymetry data using the *Surface Parameters* and *Raster Calculator* tools in ArcGIS Pro (ESRI, CA, USA) and the Benthic Terrain Modeller v3.0 plugin (Walbridge et al., 2018; Wright et al., 2005). The derivatives we used were slope, curvature, eastness, northness, relative difference from mean value (RDMV) and vector ruggedness measure (VRM) (Lecours et al., 2017; Sappington et al., 2007; Wilson et al., 2007). We selected these based on their demonstrated predictive power in the literature, their hypothesised predictive power within the context of this study, and following recommendations from Lecours et al. (2017). Morphological derivatives are typically calculated using a square window with an edge length of 3 pixels, but the scale at which they are generated and the way in which they are calculated for different scales can influence their predictive power (Misiuk et al., 2021; Porskamp et al., 2018). We define the scale of a derivative as the edge length of the square window containing the bathymetric information that influences the calculation, or the “analysis distance” *sensu* Misiuk et al. (2021). We generated all morphological derivatives at scales of 3, 6, 15, 30, 60, 100 and 140 m, an approximate geometric progression from the minimum window size up to the scale of the hydrodynamic data used (150 m, see below), beyond which we assumed predictive capability to be minimal in the context of our study. For scales of 3 m to 60 m we calculated derivatives by mean-aggregation of the bathymetry data to 2, 5, 10 and 20 m, up to the spatial precision of ground truth samples, then calculated derivatives using a 3 x 3 pixel window. For scales of 100 m and 140 m we calculated derivatives from the 20 m resolution bathymetry using 5 x 5 and 7 x 7 pixel windows. These methods of “resample-calculate” and “k x k window” are the most effective for characterising features and information at different scales (Misiuk et al., 2021). Derivatives calculated using bathymetry resolution of 1, 2, 5 and 10 m were mean-aggregated to 20 m to match the resolution of the remaining data. Multi-collinearity in predictor variables was tested and resolved by systematically removing highly collinear derivatives until the variance inflation factor for all predictors was below 10, using the *usdm* package in R (Dormann et al., 2013; Naimi et al., 2014; R Core Team, 2021) (Supporting information Fig S1). All derivative data were generated across the full extent of the bathymetry data where the k x k window contained no missing data.

To generate a predictor variable of seabed energy, we used a 3D Regional Ocean Modelling System hydrodynamic model with a horizontal resolution of 150 m and 20 vertical layers, covering the north west Wales region, derived from a larger extent model (Ward et al., 2015). The model was set to compute and output mean tidally induced bottom bed shear stress over a typical spring-neap tidal cycle (Fig. 1D). Fast tidal currents are generated at the site as the tide flows around the Isle of Anglesey and produce a local maximum of bed shear stress. Tidal current speed and bed shear stress are reduced close to the coastline and further offshore. Mean bed shear stress is a good predictor of substrate composition at regional scales (Ward et al., 2015) and is likely to have a mechanistic influence on reef substrates and benthic communities. Bathymetry for the ROMS model was provided from EMODnet (EMODnet Portal, September 2015 release) and bottom friction was controlled through a quadratic bottom drag coefficient set at 0.003 (Ward et al., 2015). Ocean boundary conditions were taken from the TOPEX/POSEIDON global tidal model (TPXO). The model validates well against the Holyhead tide gauge harmonic data (Supporting information Fig S2). We resampled the 150 m resolution bed shear stress data to 20 m using nearest neighbour without interpolation to match the spatial resolution of the morphological environmental data. As the hydrodynamic model incorporated bathymetry, and raw bathymetry within the depth range of the study site was not expected to have a mechanistic effect on benthic substrate or biogenic reef distribution, raw bathymetry was not included as a predictor variable. High quality backscatter data were not available for the full extent of the study area.

Table 2. Environmental predictor variables used to predict reef substrate and biogenic reef for each 20m x 20 m pixel in the study area after systematic removal of multi-collinear variables. *Vector ruggedness measure at 60 m scale was included in the reef substrate model but not the biogenic reef model.

Variable	Scale (m)
Curvature	3 140
Eastness	3 30 140
Northness	3 30 140
Relative difference from mean value	3 15 60 140
Slope	30 140
Vector ruggedness measure	3 15 30 60* 140
Mean bed shear stress	150

2.4 Classification model and predictive mapping

For classification and predictive mapping of reef substrate and potential biogenic reef we used Random Forests, an ensemble machine learning algorithm based on classification trees (Breiman, 2001; Cutler et al., 2007). Random Forests perform consistently well for benthic habitat mapping in a range of contexts and require minimal tuning (Mitchell et al., 2018; Wicaksono et al., 2019). The approach is non-parametric, making it a suitable choice given the characteristics of our sampling design and data. We implemented classification algorithms using the *randomForest* and *caret* packages in R (Kuhn, 2008; Liaw and Wiener, 2002; R Core Team, 2021). To estimate model performance with spatially clustered observations we implemented spatially buffered leave-one-out cross validation using the *blockCV* package (R Core Team, 2021; Valavi et al., 2019), using a buffer radius of 250 m, exceeding the median spatial autocorrelation range of our environmental predictor variables. In this method, a Random Forest model is trained on all reference data except for a test sample and the samples within a spatial buffer around it, then the model is used to predict the test sample. This is repeated using all reference samples as test samples and model performance is estimated from an error matrix of observations against predictions. Each Random Forest classification model used 1500 trees and

3 variables tested at each split, hyperparameters that we derived from preliminary tuning. We used down-sampling to balance classes in training data. The entire reference dataset was then used to train a final model to make predictions for all pixels across the study site. We mapped spatially explicit uncertainty in predictions as the model-generated probability of the predicted class for each pixel (Mitchell et al., 2018). Tree-based classifiers can resolve complicated non-linear relationships but cannot extrapolate beyond the extent of the training data. We therefore also mapped the area of applicability for the model performance estimates, outside of which the combinations of environmental predictor data were too dissimilar to the training data to be able to estimate performance (Meyer and Pebesma, 2021). To help interpret the model performance we produced plots of variable importance and partial dependence plots using the *randomForest* package. Variable importance plots show how strongly each variable influences model predictions. We used the Gini index to measure importance, describing the purity of nodes in a tree-based classifier (Breiman, 2001). Partial dependence plots visualise the influence of an individual variable on the relative likelihood that an observation will be predicted as a certain class (Friedman, 2001).

To assess the performance of a predictive mapping model, an error matrix and a selection of metrics should be considered in the context of the aims of the model and the user's interests (Foody, 2002; Olofsson et al., 2014). The error matrix documents the predicted and observed classes of the test samples, giving an estimate of the model performance for new, unknown observations. We generated a selection of standard and recommended performance metrics from the error matrix (Foody, 2002; Mitchell et al., 2018; Olofsson et al., 2014; Pontius and Millones, 2011). No single measure can fully describe performance of a classification model, but here we present balanced accuracy as an overall measure that accounts for imbalance in class prevalence (Brodersen et al., 2010). For consistency with other studies we also present overall accuracy as the proportion of correct predictions out of total predictions, and Cohen's kappa coefficient (Cohen, 1960), although their use has been discouraged (Brodersen et al., 2010; Foody, 2020; Pontius and Millones, 2011). To give context to the overall accuracy value, the no information rate is provided, equal to the proportion of the most prevalent class and therefore being the accuracy value that would be achieved by predicting all observations as one class. User's and producer's accuracies provide class-wise insight. The user's accuracy estimates the reliability of the map for a user, describing the proportion of the predictions of a class that were actually observed to be that class. The producer's accuracy, also known as sensitivity, or true positive rate, estimates the ability of a model to correctly map the land- or seascape, describing the proportion of known observations of a particular class that were correctly predicted as that class. The complement of sensitivity is specificity. Specificity, or true negative rate, describes

how many observations that were known to not be a class were correctly predicted to not be that class. Finally, we present quantity disagreement and allocation disagreement (Pontius and Millones, 2011). These measures provide information about the way in which the observations and predictions differ. High quantity disagreement indicates large differences in class prevalence while a high allocation disagreement indicates a large proportion of misclassifications. For further explanation of the metrics used see the Supporting Information.

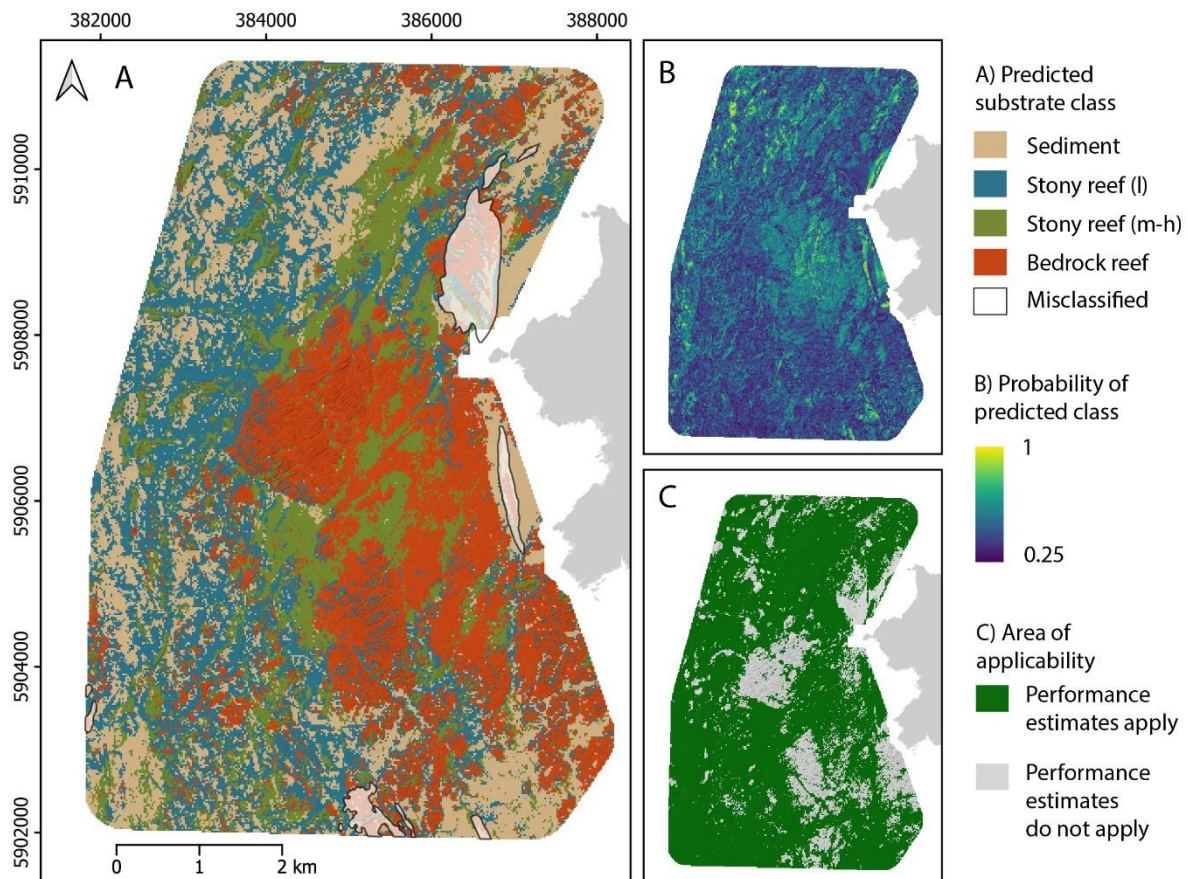


Figure 2. A) Predicted reef substrate classes with visually apparent misclassified areas are masked out. B) Probability of the predicted class for each pixel. C) Area of applicability for the performance estimates of the classifier. Areas in grey have environmental variables too dissimilar to the model training data to estimate performance.

3. Results

3.1 Reef substrate

We predicted the distribution of reef substrate in the study area by classifying the substrate into four classes: sediment (not reef), stony reef (low resemblance), stony reef (mid-high resemblance) and bedrock reef (Fig. 2A). Most observations were correctly predicted for each class (Table 3), reflected in the overall balanced accuracy of 71.7% (Table 4). For all classes, misclassifications were mostly in classes similar to the target class (Table 3). For example, sediment was mostly misclassified as stony reef (low resemblance) and rarely as bedrock. User's accuracy, estimating the reliability of the mapped pixels, was highest for stony reef (mid-high resemblance) (65.5%) and lowest for stony reef (low resemblance) (47.2%). Producer's accuracy, indicating the consistency of correctly predicting known observations, was highest for sediment (66.9%) and lowest for stony reef (low resemblance) (47.6%). The reference data and predictions differed due to misclassification (allocation disagreement = 37.2%), more than due to differences in class prevalence (quantity disagreement = 6%) (Table 4).

Table 3. Error matrix for the model predicting reef substrates following spatially buffered cross validation. True positives are in grey. Values are normalised by the total number of observations for each class, such that the columns sum to 1.

		Observed			
		Sediment	Stony reef (l)	Stony reef (m-h)	Bedrock reef
Predicted	Sediment	0.669	0.315	0.049	0.012
	Stony reef (l)	0.269	0.476	0.224	0.107
	Stony reef (m-h)	0.038	0.105	0.517	0.226
	Bedrock reef	0.023	0.105	0.210	0.655

Table 4. Performance estimates for the model predicting reef substrates following spatially buffered cross validation.

	Overall	Sediment	Stony reef (l)	Stony reef (m-h)	Bedrock reef
Total observations	500	130	143	143	84
User's accuracy	0.571	0.621	0.472	0.655	0.534
Producer's accuracy / Sensitivity	0.579	0.669	0.476	0.517	0.655
Specificity	0.855	0.857	0.787	0.891	0.885
Quantity disagreement	0.06	0.02	0.002	0.06	0.038
Allocation disagreement	0.372	0.172	0.3	0.156	0.116

Balanced accuracy	0.717
Accuracy	0.568
No information rate	0.286
Kappa	0.421

The most important variables for predicting reef substrate classes in the study area were vector ruggedness measure at scales from 3 m to 140 m, and mean bed shear stress (Fig. 3). Partial dependence plots of the three most important variables showed that areas with high fine-scale (3 m) ruggedness were more likely to be classified as bedrock and less likely to be classified as sediment, while areas with high broad-scale (140 m) ruggedness were more likely to be classified as stony reef and less likely to be classified as bedrock (Fig. 4). Areas with high mean bed shear stress (over 2.55 Nm⁻²) were more likely to be classified as bedrock or stony reef (mid-high resemblance) and less likely to be classified as sediment or stony reef (low resemblance) (Fig. 4). A reliability heat map of classification probabilities showed variation in the consistency of predictions among samples (Supporting information Figure S3).

The model predicted much of the visually rugged ground in the highest energy central region of the study area to be bedrock reef, with stony reef (mid to high resemblance) predictions concentrated in the high energy region where the ground was less rugged (Fig. 2A). A mixture of the two stony reef classes was predicted throughout the moderate energy regions where there was relatively smooth seabed and a mixture of sediment and stony reef (low resemblance) was predicted in the lowest energy regions. We could visually interpret certain seabed features like bedrock outcrops from the raw bathymetry data and qualitatively assess the performance of the predictive model for some of the study area extent. The model appeared to perform well for these areas, with most visually apparent bedrock outcrops being correctly classified. Visually apparent misclassifications were mostly concentrated around feature boundaries, but there were notable misclassifications of apparent sediment waves as bedrock. Spatially explicit classification probabilities showed that the probability of assigned classes was moderate for most of the mapped area, with a mean \pm sd of 0.47 ± 0.11 (Fig. 2B). The area of applicability analysis indicated regions of the study area where combinations of environmental variables were poorly represented in the training data and therefore model performance estimates were not reliable. The regions outside the area of applicability were mostly high energy, high ruggedness areas of apparent bedrock in the central study area and very low energy areas close to the shore in the eastern study area (Fig. 2C).

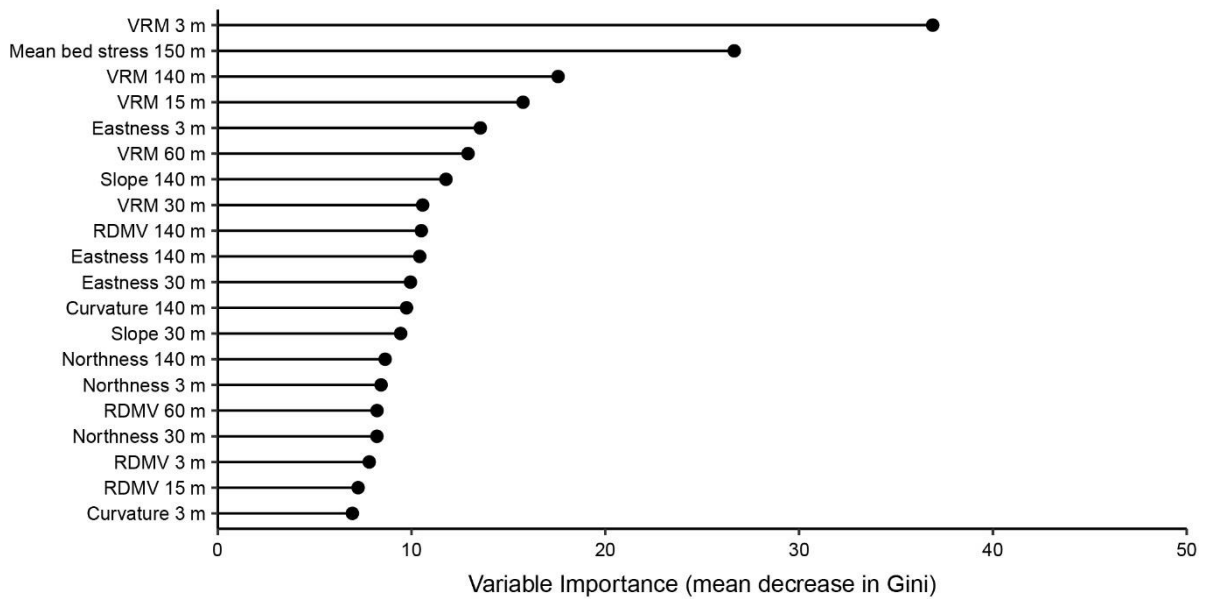


Figure 3. Relative importance of predictor variables in the model predicting reef substrate. Variable importance is quantified by the mean decrease in the Gini index if the variable is not included within the Random Forest model. The Gini index is a measure of node purity.

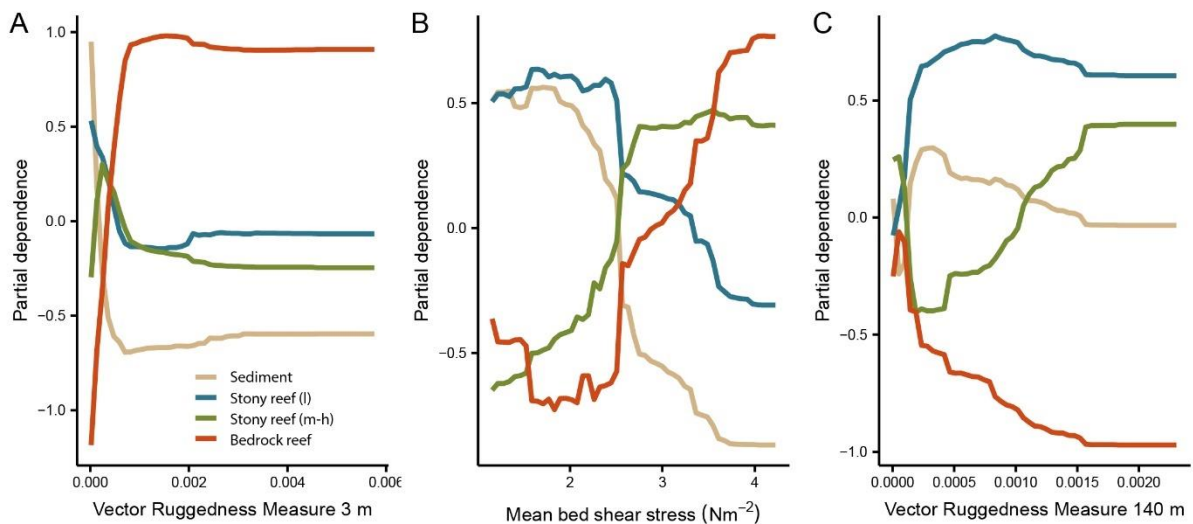


Figure 4. Partial dependence plots for the three variables with highest importance in the model predicting reef substrate. The plots visualise the influence of each variable on the likelihood that an observation is predicted to be each of four classes. For example, observations with low mean bed shear stress are less likely to be classified as bedrock reef or stony reef (mid-high resemblance) and more likely to be classified as sediment or stony reef (low resemblance).

3.2 Potential *Sabellaria spinulosa* biogenic reef

Our classification model aimed to predict two classes for *Sabellaria spinulosa*: not reef, encompassing samples with no *S. spinulosa* seen and those with *S. spinulosa* present but not forming reef, and potential reef, encompassing samples with low, medium or high resemblance to a biogenic reef. The model predicted most observations correctly with a balanced accuracy of 63.4%, but there was a high proportion of misclassifications (Table 5, Table 6). The potential reef class had a producer's accuracy of 64% but a low user's accuracy of 29.6% due to a high number of false positives (Table 6), suggesting that a map of predicted spatial distribution based on environmental variables would not be reliable. A reliability diagram indicated that the model was not well calibrated and underpredicted the potential reef class (Supporting information Figure S4).

Table 5. Error matrix for the model predicting potential *Sabellaria spinulosa* reef following spatially buffered cross validation. True positives are in grey. Values are normalised by the total number of observations for each class, such that the columns sum to 1.

		Observed	
		Not reef	Potential reef
Predicted	Not reef	0.628	0.360
	Potential reef	0.372	0.640

Table 6. Performance estimates for the model predicting potential *Sabellaria spinulosa* reef following spatially buffered cross validation.

	Overall	Not reef	Potential reef
Observations	509	409	100
User's accuracy	0.587	0.877	0.296
Producer's accuracy / Sensitivity	0.634	0.628	0.64
Specificity	0.634	0.64	0.628
Quantity disagreement	0.228	0.228	0.228
Allocation disagreement	0.141	0.141	0.141
Balanced accuracy	0.634		
Accuracy	0.631		
No information rate	0.804		
Kappa	0.187		

The variable importance plot for this model showed that mean bed shear stress was the single most important variable for predicting potential *S. spinulosa* reef, with the remaining variables having much lower importance (Fig. 5). A partial dependence plot for the effect of mean bed shear stress on class predictions showed that the potential *S. spinulosa* reef was less likely to be predicted above mean bed stress of 2.52 Nm^{-2} (Fig. 6B).

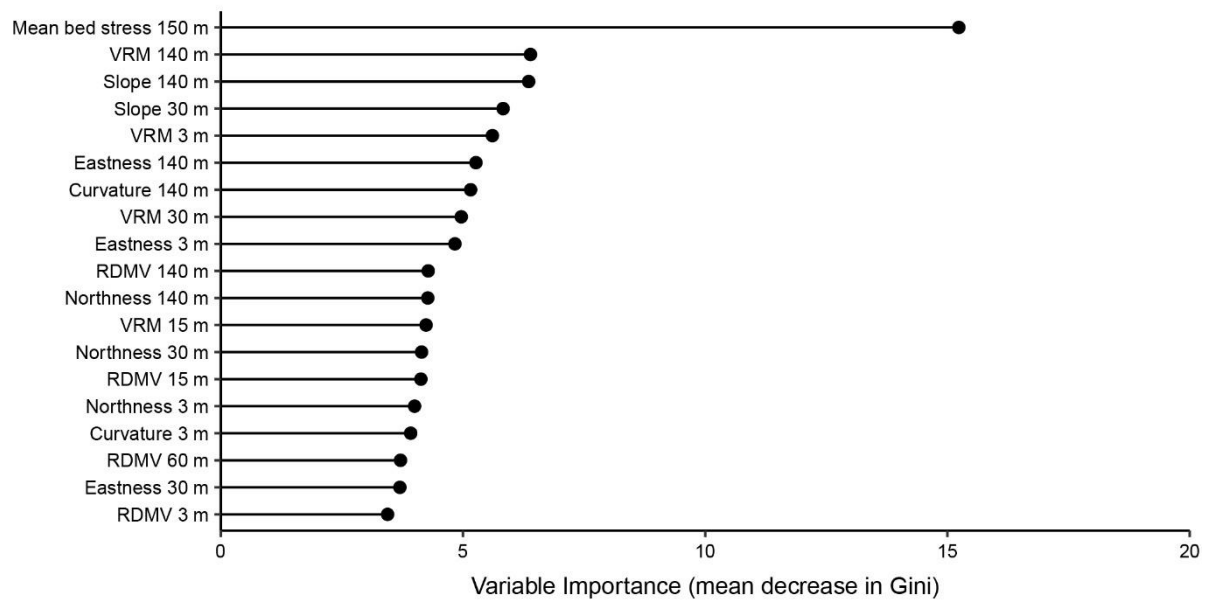


Figure 5. Relative importance of predictor variables in the model predicting potential *Sabellaria spinulosa* reef. Variable importance is quantified by the mean decrease in the Gini index if the variable is not included within the Random Forest model. The Gini index is a measure of node purity.

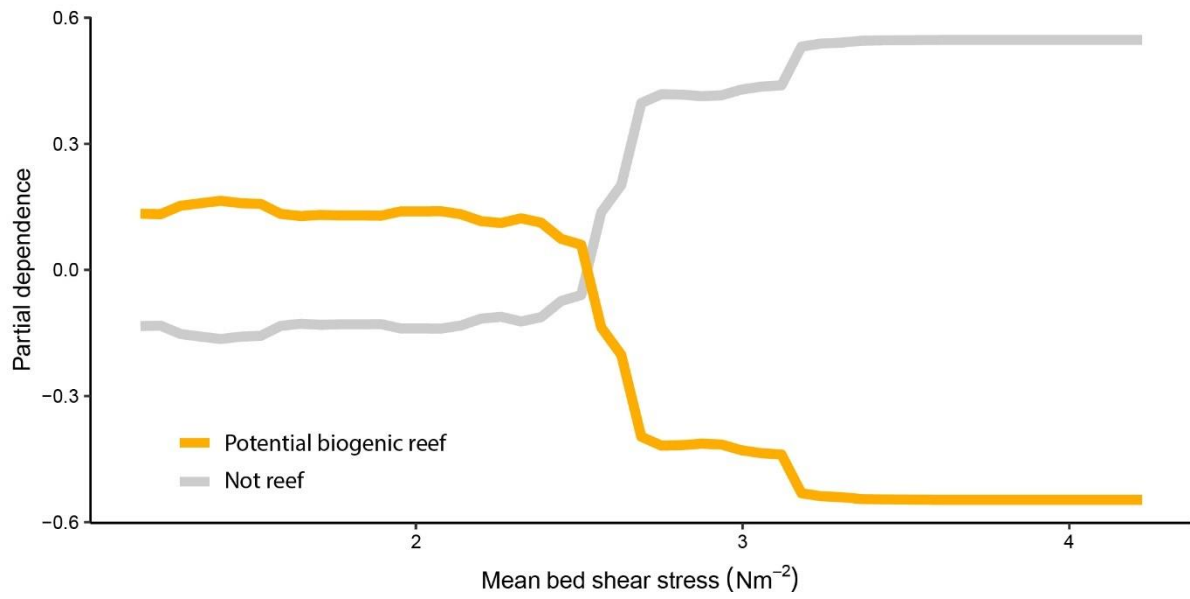


Figure 6. Partial dependence plot showing the influence of mean bed shear stress in the model predicting reef substrate. The plot visualises the influence of a single variable on the likelihood that an observation is predicted to be potential biogenic reef or not. Observations with high mean bed shear stress are less likely to be classified as potential reef and more likely to be classified as not biogenic reef.

4. Discussion

We used a machine learning approach to map previously unresolved temperate reef habitats in a high tidal energy marine region, finding that hydrodynamic energy at the seabed and ruggedness measured at multiple scales were the most important predictors of potential reef habitats. Our model predicting geogenic reef classes generated useful predictions, but our model predicting biogenic *Sabellaria spinulosa* reef did not satisfy our objectives.

Our reef substrate model performed well, with a balanced accuracy of 71.7%. The performance was sufficient to provide useful information about the distribution of potential temperate reef habitats relative to the environmental variables in our study site. While not directly comparable, other studies with similar contexts and model frameworks have reported overall accuracies of 81-93% (Haggarty and Yamanaka, 2018), and 69.7% (Porskamp et al., 2018). We were able to predict stony reef using hydrodynamic and seabed morphology data with a user's accuracy of 65.5%. As an ecologically important habitat listed in the EC Habitats Directive Annex 1, there is a need for environmental managers of member states to understand the spatial distribution of this habitat in their jurisdictional waters. Identifying and evaluating the habitat by remote sensing rather than direct observation or sampling has historically proved challenging (Irving, 2009; Limpenny et al., 2010). Our findings are encouraging and suggest that it will be possible to develop protocols to identify areas of potential stony reef using remotely sensed and modelled environmental data, enabling targeted sampling and improved efficiency in resource use for environmental management.

Mean tidally induced bed shear stress was one of the most important variables in predictive models for both reef substrate and potential *Sabellaria spinulosa* biogenic reef. Our results support findings from wave exposed coastal regions (Porskamp et al., 2018; Rattray et al., 2015), showing that hydrodynamic energy is an important predictor of reef habitats in high energy waters. Seabed ruggedness calculated at scales of 3 m, 15 m and 140 m were also important variables for predicting reef substrate. These variables had low multicollinearity indicating that they represented features of different scales in the seascape. For instance, 3 m ruggedness may represent individual boulders or topographically complex bedrock, 15 m ruggedness may represent raised patches of cobbles and boulders surrounded by more erodible sediment, and 140 m ruggedness may represent large-scale bedforms and glacial features in the region (Van Landeghem et al., 2009). Interestingly, where there was high 140 m scale ruggedness, stony reef was predicted rather than bedrock, suggesting that bedrock bathymetry was more homogenous than stony reef at this scale in our study area. Our results support an increasingly recognised need to include predictor variables at multiple scales for benthic habitat mapping (Lecours et al., 2015; Misiuk et al., 2021; Porskamp et al., 2018). As with bathymetric

indices, the ability of bed shear stress to structure and predict benthic habitats is likely to differ across spatial scales. Variation in water flow influences species distribution by controlling proximal factors across scales. For instance, suspended food availability is influenced by topographically driven turbulence at the centimetre scale (Prado et al., 2020), and by oceanographic processes like upwelling at the kilometre scale (Navarrete et al., 2005). Fine-scale hydrodynamic energy information with resolution comparable to bathymetry data across regional extents would likely enhance the performance of predictive models. This would benefit benthic habitat mapping and marine species distribution modelling to better understand patterns and processes at organism-centric scales. However, unlike bathymetry that is relatively stable through time, hydrodynamic conditions are highly variable, making simulating and validating them at fine spatial scales logistically and computationally challenging with current technology.

Our predictive model for *Sabellaria spinulosa* biogenic reef was largely driven by the singular important variable of bed shear stress. Although the performance metrics were low and the use of the model to generate a predictive map was not appropriate, the results still provide valuable insight into the environmental variables characterising *S. spinulosa* reef. *S. spinulosa* reef was not predicted to occur in the areas of the study site with highest energy, suggesting that bed shear stress was a limiting factor for the habitat above 2.52 Nm^{-2} . Higher flow rates may present barriers to larval settlement, tube building or feeding, but there is little existing information on the environmental limits of the species (Davies et al., 2009). This threshold in bed shear stress corresponded with one driving substrate predictions, above which bedrock and stony reef (mid-high resemblance) were more likely to be predicted. This may indicate that substrate suitability influenced a lack of *S. spinulosa* reef predictions in this area. While few observations of *S. spinulosa* reef on bedrock were recorded, stony reef substrate was found to support *S. spinulosa* reef in lower energy parts of the study area. There may be an interaction between substrate and bed shear stress influencing biogenic reef development that would need further research to elucidate. Bathymetric derivatives had low importance as predictor variables for potential *S. spinulosa* biogenic reef, suggesting that they were ineffective in explaining the variation in *S. spinulosa* reef presence among observations. *S. spinulosa* is difficult to detect using multibeam bathymetry acoustic data and expert interpretation of higher resolution side scan sonar data is recommended to locate potential reefs (Limpenny et al., 2010). Although our original acoustic data resolution was relatively high at 1 m, it may have still been too low to distinguish *S. spinulosa* reef morphology in a topographically variable area dominated by stony reef, and more observations of reef presence may be needed to train an effective model. Sabellariid reefs are dynamic in both space and time in terms of their emergence, density and patchiness (Jackson-

Bué et al., 2021; Jenkins et al., 2018; Pearce et al., 2014), and can survive periods of burial due to sediment transport (Hendrick et al., 2016). This presents further challenges in both detecting reef habitats and identifying its environmental niche with a limited temporal scale.

Observations through time are needed for an improved understanding of the environmental conditions suitable for *S. spinulosa* reef habitat development.

Misclassifications were identified both in the error matrices and through manual inspection of the generated predicted maps. Most misclassifications were in classes most similar to the target class, which is to be expected with a classification system that discretises the continuous variation of a natural environment (Foody, 2002; Wang, 1990). This was most evident in the low performance metrics for the stony reef (low resemblance) class, which represented an intermediate on a continuum of cobble and boulder percent cover between sediment and stony reef classes. The challenging nature of this classification task was reflected in the high proportion of relatively low pixel-wise predicted class probabilities, particularly where a mixture of sediment and stony reef classes were predicted (Fig. 2B). Continuous mapping approaches can represent gradients in natural environments better than hard classification, but at a cost of interpretability for end users (Feilhauer et al., 2020). Misclassification of sediment wave bedforms as bedrock were visually identified and could largely be explained by a paucity of observations in areas with low energy but high ruggedness. As the classification algorithm can only learn from the training data, with no rugged sediment observations in the training data, rugged ground was most likely to be predicted as bedrock or stony reef. This suggests that semi-automated and manual interpretation mapping methods are complementary and the use of multiple methods will ultimately improve the quality of benthic habitat maps (Diesing et al., 2014). Other sources of uncertainty included the limited field of view of video observations (approx. 1 x 1 m) relative to the pixel size of the final map (20 x 20 m), and the potential for the observed substrate (e.g., sediment) to be a veneer over another substrate (e.g., bedrock or biogenic reef). This is a particular concern in areas with strong tidal currents where high volumes of sediment are periodically transported and deposited during a tidal cycle and a single observation in time cannot capture such transience. Our predictive models may have been improved with multibeam echo sounder backscatter data across the extent of the study area. However, collection of high quality backscatter requires additional survey time and optimal sea state conditions, and it is an unstandardised variable (Lamarche and Lurton, 2018). Further, where a thin layer of sediment overlays hard substrate backscatter can be highly variable, making it less valuable as a predictor of observed substrate (Lucieer et al., 2013).

Accuracy metrics are useful for assessing the performance and usefulness of a model for a specific application but should not be used in isolation to compare different models and studies

(Bennett et al., 2013; Mitchell et al., 2018). The performance of benthic habitat mapping varies with decisions made throughout planning, data collection and analysis, leading to a lack of standardisation (Strong, 2020). For instance, choices in model framework, scale and choice of environmental variables, the number of observation classes used and whether to use a geomorphic or biological basis to classes, all affect different aspects of the resulting map product (Ierodionou et al., 2018; Porskamp et al., 2018; Smith et al., 2015). A predicted map should therefore be considered along with its error matrix, several performance metrics and spatially explicit uncertainty estimates in a case-by-case basis to determine its suitability for a particular user and purpose (Congalton, 1991; Foody, 2002). It should also be recognised that the performance estimates evaluate the classification model, rather than the true accuracy of a predicted map. Ideally probability sampling would be used to collect independent training and validation data for a predictive model to make design-based inference (Cochran, 1977; Olofsson et al., 2014), but this is rarely achieved for benthic mapping with resource limitations and the logistical constraints of sampling at sea, especially in high energy environments. To address the limitations of imperfect sampling design, methods have been developed to estimate a model's ability to predict into unobserved space. These include the methods applied here of spatial cross validation and area of applicability analysis (Meyer and Pebesma, 2021; Ploton et al., 2020).

The findings of this study support the use of predictive mapping as an efficient and repeatable tool for ecosystem management in logistically challenging environments like high tidal energy waters. These traditionally less anthropogenically developed and understudied regions are seeing novel industrial interest from the nascent marine renewable energy industry, generating demand for cost effective means to gather baseline ecosystem information (Shields et al., 2011; Wilding et al., 2017). We found that tidally induced seabed shear stress was a powerful variable for predicting reef habitats in high tidal energy temperate seas, and highlighted the importance of calculating bathymetric morphological derivatives at multiple scales for benthic habitat mapping. Our results will contribute to a better understanding of the spatial ecology of temperate reef ecosystems and will inform evidence-based decision making for ecosystem management in high energy marine areas.

Acknowledgements

The authors thank the Bangor University SEACAMS2 team and technical and administrative staff for supporting this research, and the crew of the RV Prince Madog for enabling the data collection. We thank Ross Griffin for facilitating access to existing data, Liz Morris-Webb for advice with benthic image analysis and Natasha Lough for advice with developing the project concept and methods. We thank the two anonymous reviewers and the Associate Editor for their comments that helped us to improve the manuscript.

Author contributions (CRediT)

TJB: Conceptualisation, methodology, software, validation, formal analysis, investigation, data curation, writing – original draft, writing – review & editing, visualisation.

GJW: Conceptualisation, methodology, writing – review & editing, supervision.

TAW: Conceptualisation, methodology, investigation, writing – review & editing.

MJR: Conceptualisation, Methodology, resources, writing – review & editing, project administration, funding acquisition.

AGB: Software, resources, data curation.

HA: Conceptualisation, methodology, validation, investigation.

JK: Conceptualisation, writing – review & editing, supervision, project administration, funding acquisition.

BP: Methodology, investigation, resources.

SJR: Resources, data curation

GLJ: Resources, project administration.

AJD: Conceptualisation, methodology, writing – review & editing, supervision.

Funding

This work formed part of the SEACAMS2 project, part-funded by the European Regional Development Fund (ERDF) through the West Wales and the Valleys Programme 2014-2020, with collaboration from Menter Môn, LL77 7LR, UK.

597 5. References

- 598 Bennett, N.D., Croke, B.F.W., Guariso, G., Guillaume, J.H.A., Hamilton, S.H., Jakeman, A.J., Marsili-
599 Libelli, S., Newham, L.T.H., Norton, J.P., Perrin, C., Pierce, S.A., Robson, B., Seppelt, R.,
600 Voinov, A.A., Fath, B.D., Andreassian, V., 2013. Characterising performance of
601 environmental models. *Environ. Model. Softw.* 40, 1–20.
602 <https://doi.org/10.1016/j.envsoft.2012.09.011>
- 603 Bennett, S., Wernberg, T., Connell, S.D., Hobday, A.J., Johnson, C.R., Poloczanska, E.S., 2016. The
604 “Great Southern Reef”: social, ecological and economic value of Australia’s neglected kelp
605 forests. *Mar. Freshw. Res.* 67, 47. <https://doi.org/10.1071/MF15232>
- 606 Breiman, L., 2001. Random forests. *Mach. Learn.* 45, 5–32.
607 <https://doi.org/10.1023/A:1010933404324>
- 608 Brodersen, K.H., Ong, C.S., Stephan, K.E., Buhmann, J.M., 2010. The balanced accuracy and its
609 posterior distribution, in: *Proceedings - International Conference on Pattern Recognition*.
610 pp. 3121–3124. <https://doi.org/10.1109/ICPR.2010.764>
- 611 Brown, C.J., Smith, S.J., Lawton, P., Anderson, J.T., 2011. Benthic habitat mapping: A review of
612 progress towards improved understanding of the spatial ecology of the seafloor using
613 acoustic techniques. *Estuar. Coast. Shelf Sci.* 92, 502–520.
614 <https://doi.org/10.1016/j.ecss.2011.02.007>
- 615 Bué, M., Smale, D.A., Natanni, G., Marshall, H., Moore, P.J., 2020. Multiple-scale interactions
616 structure macroinvertebrate assemblages associated with kelp understory algae. *Divers.*
617 *Distrib.* 26, 1551–1565. <https://doi.org/10.1111/ddi.13140>
- 618 Cochran, W.G., 1977. *Sampling Techniques*, 3rd ed. John Wiley & Sons.
- 619 Cogan, C.B., Todd, B.J., Lawton, P., Noji, T.T., 2009. The role of marine habitat mapping in
620 ecosystem-based management. *ICES J. Mar. Sci.* 66, 2033–2042.
621 <https://doi.org/10.1093/icesjms/fsp214>
- 622 Coggan, R., Barrio Froján, C.R.S., Diesing, M., Aldridge, J., 2012. Spatial patterns in gravel habitats
623 and communities in the central and eastern English Channel. *Estuar. Coast. Shelf Sci.* 111,
624 118–128. <https://doi.org/10.1016/j.ecss.2012.06.017>
- 625 Cohen, J., 1960. A Coefficient of Agreement for Nominal Scales. *Educ. Psychol. Meas.* 20, 37–46.
626 <https://doi.org/10.1177/001316446002000104>
- 627 Congalton, R.G., 1991. A review of assessing the accuracy of classifications of remotely sensed
628 data. *Remote Sens. Environ.* 37, 35–46. [https://doi.org/10.1016/0034-4257\(91\)90048-B](https://doi.org/10.1016/0034-4257(91)90048-B)
- 629 Cowen, R.K., Sponaugle, S., 2009. Larval Dispersal and Marine Population Connectivity. *Ann. Rev.*
630 *Mar. Sci.* 1, 443–466. <https://doi.org/10.1146/annurev.marine.010908.163757>
- 631 Cutler, D.R., Edwards, T.C., Beard, K.H., Cutler, A., Hess, K.T., Gibson, J., Lawler, J.J., 2007. Random
632 forests for classification in ecology. *Ecology* 88, 2783–2792. <https://doi.org/10.1890/07-0539.1>
- 634 D’Urban Jackson, T., Williams, G.J., Walker-Springett, G., Davies, A.J., 2020. Three-dimensional
635 digital mapping of ecosystems: A new era in spatial ecology. *Proc. R. Soc. B Biol. Sci.* 287, 1–
636 10. <https://doi.org/10.1098/rspb.2019.2383>
- 637 Dalkin, M., 2008. Mid Irish Sea reefs habitat mapping report. *Eur. Environ. Agency* 306.
- 638 Dannheim, J., Bergström, L., Birchenough, S.N.R., Brzana, R., Boon, A.R., Coolen, J.W.P., Dauvin,
639 J.C., De Mesel, I., Derweduwen, J., Gill, A.B., Hutchison, Z.L., Jackson, A.C., Janas, U., Martin, G.,

640 Raoux, A., Reubens, J., Rostin, L., Vanaverbeke, J., Wilding, T.A., Wilhelmsson, D., Degraer, S.,
641 2020. Benthic effects of offshore renewables: Identification of knowledge gaps and
642 urgently needed research. ICES J. Mar. Sci. 77, 1092–1108.
643 <https://doi.org/10.1093/icesjms/fsz018>

644 Davies, A.J., Guinotte, J.M., 2011. Global Habitat Suitability for Framework-Forming Cold-Water
645 Corals. PLoS One 6, e18483. <https://doi.org/10.1371/journal.pone.0018483>

646 Davies, A.J., Last, K.S., Attard, K., Hendrick, V.J., 2009. Maintaining turbidity and current flow in
647 laboratory aquarium studies, a case study using *Sabellaria spinulosa*. J. Exp. Mar. Bio. Ecol.
648 370, 35–40. <https://doi.org/10.1016/j.jembe.2008.11.015>

649 Diesing, M., Coggan, R., Vanstaen, K., 2009. Widespread rocky reef occurrence in the central
650 English Channel and the implications for predictive habitat mapping. Estuar. Coast. Shelf
651 Sci. 83, 647–658. <https://doi.org/10.1016/j.ecss.2009.05.018>

652 Diesing, M., Green, S.L., Stephens, D., Lark, R.M., Stewart, H.A., Dove, D., 2014. Mapping seabed
653 sediments: Comparison of manual, geostatistical, object-based image analysis and machine
654 learning approaches. Cont. Shelf Res. 84, 107–119.
655 <https://doi.org/10.1016/j.csr.2014.05.004>

656 Dormann, C.F., Elith, J., Bacher, S., Buchmann, C., Carl, G., Carré, G., Marquéz, J.R.G., Gruber, B.,
657 Lafourcade, B., Leitão, P.J., Münkemüller, T., McClean, C., Osborne, P.E., Reineking, B.,
658 Schröder, B., Skidmore, A.K., Zurell, D., Lautenbach, S., 2013. Collinearity: a review of
659 methods to deal with it and a simulation study evaluating their performance. Ecography
660 (Cop.). 36, 27–46. <https://doi.org/10.1111/j.1600-0587.2012.07348.x>

661 Eckman, J.E., Duggins, D.O., 1993. Effects of Flow Speed on Growth of Benthic Suspension
662 Feeders. Biol. Bull. 185, 28–41. <https://doi.org/10.2307/1542128>

663 Eggleton, J., Meadows, W., 2013. Offshore monitoring of Annex I reef habitat present within the
664 Isles of Scilly Special Area of Conservation (SAC). Natural England Commissioned Report
665 NECR125.

666 European Commission, 2013. Interpretation Manual of European Union Habitats.
667 [https://doi.org/10.1016/S0021-9290\(99\)00083-4](https://doi.org/10.1016/S0021-9290(99)00083-4)

668 Feilhauer, H., Zlinszky, A., Kania, A., Foody, G.M., Doktor, D., Lausch, A., Schmidtlein, S., 2020. Let
669 your maps be fuzzy!—Class probabilities and floristic gradients as alternatives to crisp
670 mapping for remote sensing of vegetation. Remote Sens. Ecol. Conserv. rse2.188.
671 <https://doi.org/10.1002/rse2.188>

672 Foody, G.M., 2020. Explaining the unsuitability of the kappa coefficient in the assessment and
673 comparison of the accuracy of thematic maps obtained by image classification. Remote
674 Sens. Environ. 239, 111630. <https://doi.org/10.1016/j.rse.2019.111630>

675 Foody, G.M., 2002. Status of land cover classification accuracy assessment. Remote Sens.
676 Environ. 80, 185–201. [https://doi.org/10.1016/S0034-4257\(01\)00295-4](https://doi.org/10.1016/S0034-4257(01)00295-4)

677 Friedman, J.H., 2001. Greedy Function Approximation: A Gradient Boosting Machine 29, 1189–
678 1232.

679 Gove, J.M., Williams, G.J., McManus, M.A., Clark, S.J., Ehses, J.S., Wedding, L.M., 2015. Coral reef
680 benthic regimes exhibit non-linear threshold responses to natural physical drivers. Mar.
681 Ecol. Prog. Ser. 522, 33–48. <https://doi.org/10.3354/MEPS11118>

682 Gutiérrez, D., Enríquez, E., Purca, S., Quipúzcoa, L., Marquina, R., Flores, G., Graco, M., 2008.
683 Oxygenation episodes on the continental shelf of central Peru: Remote forcing and benthic
684 ecosystem response. Prog. Oceanogr. 79, 177–189.

685 <https://doi.org/10.1016/j.pocean.2008.10.025>

686 Haggarty, D., Yamanaka, L., 2018. Evaluating Rockfish Conservation Areas in southern British
687 Columbia, Canada using a Random Forest model of rocky reef habitat. *Estuar. Coast. Shelf*
688 *Sci.* 208, 191–204. <https://doi.org/10.1016/j.ecss.2018.05.011>

689 Hendrick, V.J., Foster-Smith, R.L., 2006. *Sabellaria spinulosa* reef: A scoring system for evaluating
690 “reefiness” in the context of the Habitats Directive. *J. Mar. Biol. Assoc. United Kingdom* 86,
691 665–677. <https://doi.org/10.1017/S0025315406013555>

692 Hendrick, V.J., Hutchison, Z.L., Last, K.S., 2016. Sediment burial intolerance of marine
693 macroinvertebrates. *PLoS One* 11, 149114.
694 <https://doi.org/10.1371/journal.pone.0149114>

695 Holbrook, S.J., Schmitt, R.J., Ambrose, R.F., 1990. Biogenic habitat structure and characteristics of
696 temperate reef fish assemblages. *Aust. J. Ecol.* 15, 489–503.
697 <https://doi.org/10.1111/j.1442-9993.1990.tb01473.x>

698 Holt, T., Rees, E., Hawkins, S., Seed, R., 1998. Biogenic Reefs (volume IX). An overview of dynamic
699 and sensitivity characteristics for conservation management of marine SACs. Scottish
700 Association for Marine Science (UK Marine SACs Project).

701 Huang, Z., Brooke, B.P., Harris, P.T., 2011. A new approach to mapping marine benthic habitats
702 using physical environmental data. *Cont. Shelf Res.* 31, S4–S16.
703 <https://doi.org/10.1016/j.csr.2010.03.012>

704 Ierodiaconou, D., Schimel, A.C.G., Kennedy, D., Monk, J., Gaylard, G., Young, M., Diesing, M.,
705 Rattray, A., 2018. Combining pixel and object based image analysis of ultra-high resolution
706 multibeam bathymetry and backscatter for habitat mapping in shallow marine waters.
707 *Mar. Geophys. Res.* 39, 271–288. <https://doi.org/10.1007/s11001-017-9338-z>

708 Irving, R., 2009. The identification of the main characteristics of stony reef habitats under the
709 Habitats Directive. *JNCC Rep. No.* 432 44.

710 Jackson-Bué, T., Williams, G.J., Walker-Springett, G., Rowlands, S.J., Davies, A.J., 2021. Three-
711 dimensional mapping reveals scale-dependent dynamics in biogenic reef habitat structure.
712 *Remote Sens. Ecol. Conserv.* <https://doi.org/10.1002/RSE2.213>

713 Jenkins, C., Eggleton, J., Barry, J., O’Connor, J., 2018. Advances in assessing *Sabellaria spinulosa*
714 reefs for ongoing monitoring. *Ecol. Evol.* 8, 7673–7687.
715 <https://doi.org/10.1002/ece3.4292>

716 Jouffray, J.B., Blasiak, R., Norström, A. V., Österblom, H., Nyström, M., 2020. The Blue
717 Acceleration: The Trajectory of Human Expansion into the Ocean. *One Earth* 2, 43–54.
718 <https://doi.org/10.1016/j.ONEEAR.2019.12.016>

719 Kerr, J.T., Ostrovsky, M., 2003. From space to species: Ecological applications for remote sensing.
720 *Trends Ecol. Evol.* 18, 299–305. [https://doi.org/10.1016/S0169-5347\(03\)00071-5](https://doi.org/10.1016/S0169-5347(03)00071-5)

721 Koehl, M.A.R., 1999. Ecological biomechanics of benthic organisms. *J. Exp. Biol.* 202, 3469–3476.

722 Kuhn, M., 2008. Building Predictive Models in R Using the caret Package. *J. Stat. Softw.* 28, 1–26.
723 <https://doi.org/10.18637/JSS.V028.I05>

724 Lamarche, G., Lurton, X., 2018. Recommendations for improved and coherent acquisition and
725 processing of backscatter data from seafloor-mapping sonars. *Mar. Geophys. Res.* 39, 5–22.
726 <https://doi.org/10.1007/s11001-017-9315-6>

727 Lecours, V., Devillers, R., Schneider, D.C., Lucieer, V.L., Brown, C.J., Edinger, E.N., 2015. Spatial
728 scale and geographic context in benthic habitat mapping: Review and future directions.

729 Mar. Ecol. Prog. Ser. 535, 259–284. <https://doi.org/10.3354/meps11378>

730 Lecours, V., Devillers, R., Simms, A.E., Lucieer, V.L., Brown, C.J., 2017. Towards a framework for
731 terrain attribute selection in environmental studies. *Environ. Model. Softw.* 89, 19–30.
732 <https://doi.org/10.1016/j.envsoft.2016.11.027>

733 Liaw, A., Wiener, M., 2002. Classification and Regression by randomForest. *R News* 2, 18–22.

734 Limpenny, D.S., Foster-Smith, R.L., Edwards, T.M., Hendrick, V.J., Diesing, M., Eggleton, J.D.,
735 Meadows, W.J., Crutchfield, Z., Pfeifer, S., Reach, I.S., 2010. Best methods for identifying and
736 evaluating *Sabellaria spinulosa* and cobble reef. Aggregate Levy Sustainability Fund Project
737 MAL0008 134.

738 Lindenbaum, C., Bennell, J.D., Rees, E.I.S., Mcclean, D., Cook, W., Wheeler, A.J., Sanderson, W.G.,
739 2008. Small-scale variation within a *Modiolus modiolus* (Mollusca: Bivalvia) reef in the Irish
740 Sea: I. Seabed mapping and reef morphology. *J. Mar. Biol. Assoc. United Kingdom* 88, 133–
741 141. <https://doi.org/10.1017/S0025315408000374>

742 Lucieer, V., Hill, N.A., Barrett, N.S., Nichol, S., 2013. Do marine substrates “look” and “sound” the
743 same? Supervised classification of multibeam acoustic data using autonomous underwater
744 vehicle images. *Estuar. Coast. Shelf Sci.* 117, 94–106.
745 <https://doi.org/10.1016/j.ecss.2012.11.001>

746 MarineSpace, 2019. Morlais Project Environmental Statement Chapter 9 : Benthic and Intertidal
747 Ecology Volume I.

748 Mayer, L., Jakobsson, M., Allen, G., Dorschel, B., Falconer, R., Ferrini, V., Lamarche, G., Snaith, H.,
749 Weatherall, P., 2018. The Nippon Foundation—GEBCO Seabed 2030 Project: The Quest to
750 See the World’s Oceans Completely Mapped by 2030. *Geosciences* 8, 63.
751 <https://doi.org/10.3390/geosciences8020063>

752 McDermid, G.J., Franklin, S.E., LeDrew, E.F., 2005. Remote sensing for large-area habitat
753 mapping. *Prog. Phys. Geogr. Earth Environ.* 29, 449–474.
754 <https://doi.org/10.1191/0309133305pp455ra>

755 Meyer, H., Pebesma, E., 2021. Predicting into unknown space? Estimating the area of
756 applicability of spatial prediction models. *Methods Ecol. Evol.* 12, 1620–1633.
757 <https://doi.org/10.1111/2041-210X.13650>

758 Misiuk, B., Lecours, V., Dolan, M.F.J., Robert, K., 2021. Evaluating the Suitability of Multi-Scale
759 Terrain Attribute Calculation Approaches for Seabed Mapping Applications. *Mar. Geod.* 44,
760 327–385. <https://doi.org/10.1080/01490419.2021.1925789>

761 Mitchell, P.J., Downie, A.L., Diesing, M., 2018. How good is my map? A tool for semi-automated
762 thematic mapping and spatially explicit confidence assessment. *Environ. Model. Softw.* 108,
763 111–122. <https://doi.org/10.1016/j.envsoft.2018.07.014>

764 Naimi, B., Hamm, N.A.S., Groen, T.A., Skidmore, A.K., Toxopeus, A.G., 2014. Where is positional
765 uncertainty a problem for species distribution modelling? *Ecography (Cop.)*. 37, 191–203.
766 <https://doi.org/10.1111/j.1600-0587.2013.00205.x>

767 Navarrete, S.A., Wieters, E.A., Broitman, B.R., Castilla, J.C., 2005. Scales of benthic-pelagic
768 coupling and the intensity of species interactions: From recruitment limitation to top-
769 down control. *Proc. Natl. Acad. Sci. U. S. A.* 102, 18046–18051.
770 <https://doi.org/10.1073/pnas.0509119102>

771 Olofsson, P., Foody, G.M., Herold, M., Stehman, S. V., Woodcock, C.E., Wulder, M.A., 2014. Good
772 practices for estimating area and assessing accuracy of land change. *Remote Sens. Environ.*
773 148, 42–57. <https://doi.org/10.1016/j.rse.2014.02.015>

774 Pearce, B., 2017. The ecology of *Sabellaria spinulosa* reefs. Plymouth University.

775 Pearce, B., Fariñas-Franco, J.M., Wilson, C., Pitts, J., DeBurgh, A., Somerfield, P.J., 2014. Repeated
776 mapping of reefs constructed by *Sabellaria spinulosa* Leuckart 1849 at an offshore wind
777 farm site. Cont. Shelf Res. 83, 3–13. <https://doi.org/10.1016/j.csr.2014.02.003>

778 Pearman, T.R.R., Robert, K., Callaway, A., Hall, R., Lo Iacono, C., Huvenne, V.A.I., 2020. Improving
779 the predictive capability of benthic species distribution models by incorporating
780 oceanographic data – Towards holistic ecological modelling of a submarine canyon. Prog.
781 Oceanogr. 184. <https://doi.org/10.1016/j.pocean.2020.102338>

782 Plets, R., Clements, A., Quinn, R., Strong, J., Breen, J., Edwards, H., 2012. Marine substratum map
783 of the Causeway Coast, Northern Ireland. J. Maps 8, 1–13.
784 <https://doi.org/10.1080/17445647.2012.661957>

785 Ploton, P., Mortier, F., Réjou-Méchain, M., Barbier, N., Picard, N., Rossi, V., Dormann, C., Cornu, G.,
786 Viennois, G., Bayol, N., Lyapustin, A., Gourlet-Fleury, S., Pélissier, R., 2020. Spatial validation
787 reveals poor predictive performance of large-scale ecological mapping models. Nat.
788 Commun. 11, 1–11. <https://doi.org/10.1038/s41467-020-18321-y>

789 Pontius, R.G., Millones, M., 2011. Death to Kappa: birth of quantity disagreement and allocation
790 disagreement for accuracy assessment.
791 <http://dx.doi.org/10.1080/01431161.2011.552923> 32, 4407–4429.
792 <https://doi.org/10.1080/01431161.2011.552923>

793 Porskamp, P., Rattray, A., Young, M., Ierodiaconou, D., 2018. Multiscale and hierarchical
794 classification for benthic habitat mapping. Geosci. 8.
795 <https://doi.org/10.3390/geosciences8040119>

796 Prado, E., Rodríguez-Basalo, A., Cobo, A., Ríos, P., Sánchez, F., 2020. 3D fine-scale terrain
797 variables from underwater photogrammetry: A new approach to benthic microhabitat
798 modeling in a circalittoral Rocky shelf. Remote Sens. 12, 2466.
799 <https://doi.org/10.3390/RS12152466>

800 R Core Team, 2021. R: A Language and Environment for Statistical Computing.

801 Rattray, A., Ierodiaconou, D., Womersley, T., 2015. Wave exposure as a predictor of benthic
802 habitat distribution on high energy temperate reefs. Front. Mar. Sci. 2, 8.
803 <https://doi.org/10.3389/fmars.2015.00008>

804 Robinson, K.A., Ramsay, K., Lindenbaum, C., Frost, N., Moore, J., Wright, A.P., Petrey, D., 2011.
805 Predicting the distribution of seabed biotopes in the southern Irish Sea. Cont. Shelf Res. 31,
806 S120–S131. <https://doi.org/10.1016/j.csr.2010.01.010>

807 Roche, R.C., Walker-Springett, K., Robins, P.E., Jones, J., Veneruso, G., Whitton, T.A., Piano, M.,
808 Ward, S.L., Duce, C.E., Waggitt, J.J., Walker-Springett, G.R., Neill, S.P., Lewis, M.J., King, J.W.,
809 2016. Research priorities for assessing potential impacts of emerging marine renewable
810 energy technologies: Insights from developments in Wales (UK). Renew. Energy 99, 1327–
811 1341. <https://doi.org/10.1016/j.renene.2016.08.035>

812 Rosenberg, R., 1995. Benthic marine fauna structured by hydrodynamic processes and food
813 availability. Netherlands J. Sea Res. 34, 303–317. [https://doi.org/10.1016/0077-7579\(95\)90040-3](https://doi.org/10.1016/0077-7579(95)90040-3)

815 Royal Haskoning DHV, 2019. Morlais Project Environmental Statement Chapter 7 : Metocean
816 Conditions and Coastal Processes Volume I.

817 Sappington, J.M., Longshore, K.M., Thompson, D.B., 2007. Quantifying Landscape Ruggedness for
818 Animal Habitat Analysis: A Case Study Using Bighorn Sheep in the Mojave Desert. J. Wildl.

819 Manage. 71, 1419–1426. <https://doi.org/10.2193/2005-723>

820 Sebens, K.P., Grace, S.P., Helmuth, B., Maney, E.J., Miles, J.S., 1998. Water flow and prey capture
821 by three scleractinian corals, *Madracis mirabilis*, *Montastrea cavernosa* and *Porites porites*
822 in a field enclosure. Mar. Biol. 131, 347–360. <https://doi.org/10.1007/s002270050328>

823 Shields, A., 1936. Anwendung der Aehnlichkeitsmechanik und der Turbulenzforschung auf die
824 Geschiebebewegung. Technical University Berlin.

825 Shields, M.A., Woolf, D.K., Grist, E.P.M., Kerr, S.A., Jackson, A.C., Harris, R.E., Bell, M.C., Beharie, R.,
826 Want, A., Osalusi, E., Gibb, S.W., Side, J., 2011. Marine renewable energy: The ecological
827 implications of altering the hydrodynamics of the marine environment. Ocean Coast.
828 Manag. 54, 2–9. <https://doi.org/10.1016/J.OCECOAMAN.2010.10.036>

829 Smith, J., O'Brien, P.E., Stark, J.S., Johnstone, G.J., Riddle, M.J., 2015. Integrating multibeam sonar
830 and underwater video data to map benthic habitats in an East Antarctic nearshore
831 environment. Estuar. Coast. Shelf Sci. 164, 520–536.
832 <https://doi.org/10.1016/j.ecss.2015.07.036>

833 Strong, J.A., 2020. An error analysis of marine habitat mapping methods and prioritised work
834 packages required to reduce errors and improve consistency. Estuar. Coast. Shelf Sci. 240,
835 106684. <https://doi.org/10.1016/j.ecss.2020.106684>

836 Taylor, R., 1998. Density, biomass and productivity of animals in four subtidal rocky reef
837 habitats: the importance of small mobile invertebrates. Mar. Ecol. Prog. Ser. 172, 37–51.
838 <https://doi.org/10.3354/meps172037>

839 Turner, M.G., 1989. Landscape ecology: the effect of pattern on process. Annu. Rev. Ecol. Syst. 20,
840 171–197. <https://doi.org/10.1146/annurev.es.20.110189.001131>

841 Valavi, R., Elith, J., Lahoz-Monfort, J.J., Guillera-Arroita, G., 2019. blockCV: An r package for
842 generating spatially or environmentally separated folds for k-fold cross-validation of
843 species distribution models. Methods Ecol. Evol. 10, 225–232.
844 <https://doi.org/10.1111/2041-210X.13107>

845 Van Landeghem, K.J.J., Wheeler, A.J., Mitchell, N.C., 2009. Seafloor evidence for palaeo-ice
846 streaming and calving of the grounded Irish Sea Ice Stream: Implications for the
847 interpretation of its final deglaciation phase. Boreas 38, 119–131.
848 <https://doi.org/10.1111/J.1502-3885.2008.00041.X>

849 van Rein, H.B., Brown, C., Quinn, R., Breen, J., 2009. A review of sublittoral monitoring methods
850 in temperate waters: A focus on scale. Underw. Technol. 28, 99–113.
851 <https://doi.org/10.3723/ut.28.099>

852 Vanstaen, K., Eggleton, J., 2011. Mapping Annex 1 reef habitat present in specific areas within
853 the Lyme Bay and Torbay cSAC. Cefas report C5291B.

854 Walbridge, S., Slocum, N., Pobuda, M., Wright, D.J., 2018. Unified geomorphological analysis
855 workflows with benthic terrain modeler. Geosci. 8.
856 <https://doi.org/10.3390/geosciences8030094>

857 Wang, F., 1990. Fuzzy Supervised Classification of Remote Sensing Images. IEEE Trans. Geosci.
858 Remote Sens. 28, 194–201. <https://doi.org/10.1109/36.46698>

859 Ward, S.L., Neill, S.P., Van Landeghem, K.J.J., Scourse, J.D., 2015. Classifying seabed sediment type
860 using simulated tidal-induced bed shear stress. Mar. Geol. 367, 94–104.
861 <https://doi.org/10.1016/j.margeo.2015.05.010>

862 Warrens, M.J., 2015. Properties of the quantity disagreement and the allocation disagreement.

863 <http://dx.doi.org/10.1080/01431161.2015.1011794> 36, 1439–1446.
864 <https://doi.org/10.1080/01431161.2015.1011794>

865 Warwick, R., Uncles, R., 1980. Distribution of Benthic Macrofauna Associations in the Bristol
866 Channel in Relation to Tidal Stress. *Mar. Ecol. Prog. Ser.* 3, 97–103.
867 <https://doi.org/10.3354/meps003097>

868 Whitton, T., 2014. Characterization of the benthic habitats in the West Anglesey Demonstration
869 Zone. SEACAMS report SC-RD-116.

870 Wicaksono, P., Aryaguna, P.A., Lazuardi, W., 2019. Benthic Habitat Mapping Model and Cross
871 Validation Using Machine-Learning Classification Algorithms. *Remote Sens.* 11, 1279.
872 <https://doi.org/10.3390/rs11111279>

873 Wilding, T.A., Gill, A.B., Boon, A., Sheehan, E., Dauvin, J., Pezy, J.-P., O’Beirn, F., Janas, U., Rostin, L.,
874 De Mesel, I., 2017. Turning off the DRIP (‘Data-rich, information-poor’) – rationalising
875 monitoring with a focus on marine renewable energy developments and the benthos.
876 *Renew. Sustain. Energy Rev.* 74, 848–859. <https://doi.org/10.1016/j.rser.2017.03.013>

877 Wilson, M.F.J., O’Connell, B., Brown, C., Guinan, J.C., Grehan, A.J., 2007. Multiscale Terrain
878 Analysis of Multibeam Bathymetry Data for Habitat Mapping on the Continental Slope. *Mar.*
879 *Geod.* 30, 3–35. <https://doi.org/10.1080/01490410701295962>

880 Wright, D.J., Lundblad, E.R., Larkin, E.M., Rinehart, R.W., Murphy, J., Cary-Kothera, L., Draganov,
881 K., 2005. ArcGIS Benthic Terrain Modeler.

882

883

Supporting information

Accuracy metrics

No single metric can fully describe the accuracy of a predictive map. To assess the accuracy of a predictive map for a specific purpose, a selection of accuracy estimates should be considered that are derived from the error matrix of predictions and observations. The error matrix is also known as a confusion matrix or contingency table. In this paper we use some of the more common metrics found in the literature. Here, we describe how the metrics we used were calculated using a generic example error matrix with three classes.

Metric: **Overall accuracy**

Synonyms: Accuracy

Description: The proportion of correct positive predictions.

Calculation: $\text{True positives (all classes)} / \text{Total observations (all classes)}$

		Observed			
Predicted		A	B	C	Totals
	A	22	7	0	29
	B	4	39	9	52
	C	2	5	12	19
Totals		28	51	21	100

Overall accuracy = 0.73

Metric: **User's accuracy**

Synonyms: Error of commission, precision, positive predictive value

Description: For a specific class, the proportion of positive predictions that were observed to be that class.

Calculation: $\text{True positives (Class A)} / \text{Total predictions (Class A)}$

		Observed			
Predicted		A	B	C	Totals
	A	22	7	0	29
	B	4	39	9	52
	C	2	5	12	19
Totals		28	51	21	100

User's accuracy (Class A) = 0.76

Metric: **Producer's accuracy / Sensitivity**

Synonyms: Error of omission, true positive rate, recall

Description: For a specific class, what proportion of positive observations were correctly predicted?

Calculation: $\frac{\text{True positives (Class A)}}{\text{Total observations (Class A)}}$

		Observed			Totals
		A	B	C	
Predicted	A	22	7	0	29
	B	4	39	9	52
	C	2	5	12	19
	Totals	28	51	21	100

$\text{Producer's accuracy / Sensitivity (Class A)} = 0.79$

Metric: **Specificity**

Synonyms: True negative rate

Description: For a specific class, what proportion of negative observations were correctly predicted?

Calculation: $\frac{\text{True negatives (Class A)}}{\text{Total negative observations (Class A)}}$

		Observed			Totals
		A	B	C	
Predicted	A	22	7	0	29
	B	4	39	9	52
	C	2	5	12	19
	Totals	28	51	21	100

$\text{Specificity (Class A)} = 0.90$

Metric: **Balanced accuracy**

Description: An overall accuracy metric that compensates for unbalanced class observations

Calculation: The global mean of the class-wise means of sensitivity and specificity

$$\frac{((\text{Sensitivity (Class A)} + \text{Specificity (Class A)}) / 2) + ((\text{Sensitivity (Class B)} + \text{Specificity (Class B)}) / 2) + ((\text{Sensitivity (Class C)} + \text{Specificity (Class C)}) / 2)}{3}$$

929

930 **Metric: Quantity disagreement**

931 Description: Error attributed to differences in the class prevalence of observations and
932 predictions (Pontius and Millones, 2011; Warrens, 2015).

933 Calculation: Where p_{ij} is the proportion of samples observed as class i and predicted as class j ,
934 p_{i+} and p_{+i} are the observed and predicted totals for each class respectively, or the column and
935 row totals of an error matrix of the proportions, such that the full matrix sums to 1, and c is the
936 number of classes (Warrens, 2015)

937

938 The quantity disagreement of class i is given by

939

940
$$q_i = |p_{i+} - p_{+i}|$$

941

942 The overall quantity disagreement is given by

943

944
$$Q = \frac{1}{2} \sum_{i=1}^c |p_{i+} - p_{+i}|$$

945

946 **Metric: Allocation disagreement**

947 Description: Error attributed to differences in per-unit class identities between observations
948 and predictions (Pontius and Millones, 2011; Warrens, 2015).

949 Calculation: Using the definitions given for quantity disagreement (Warrens, 2015)

950

951 The allocation disagreement for class i is given by

952

953
$$a_i = 2 \min(p_{i+}, p_{+i}) - 2p_{ii}$$

954

955 The overall allocation disagreement is given by

956

957
$$A = \left[\sum_{i=1}^c \min(p_{i+}, p_{+i}) \right] - \sum_{i=1}^c p_{ii}$$

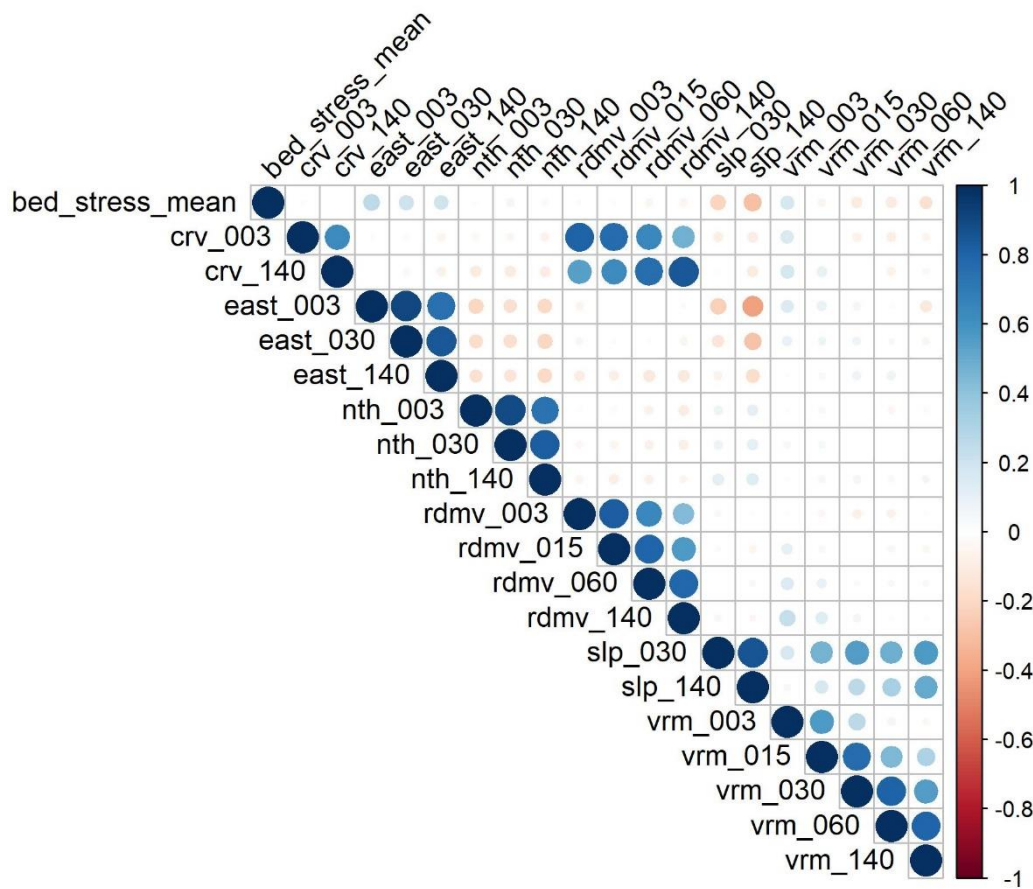


Figure S1. Correlation matrix of environmental predictor variables included in the predictive models. Circle colour and size indicate the strength and sign of correlation between two variables. Morphological variable names include the derivative abbreviation and scale (m). Abberviations: curvature (crv), eastness (east), northness (nth), relative difference from mean value (rdmv), slope (slp), vector ruggedness measure (vrm). Vrm_60 was included in the substrate model but not the *Sabellaria spinulosa* model after variable selection by variance inflation factor.

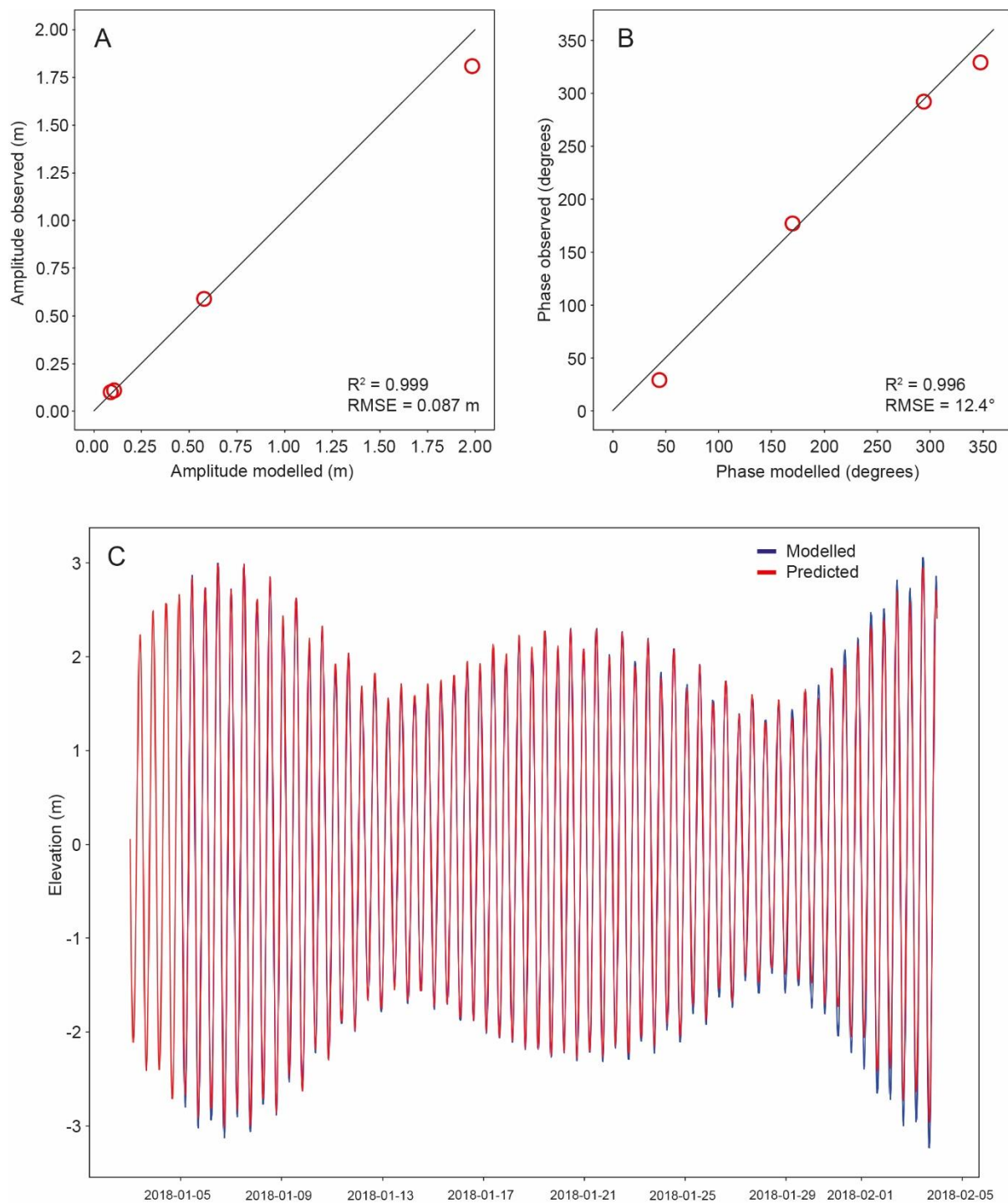


Figure S2. Our hydrodynamic model validates well against Holyhead tidal gauge harmonic data in amplitude (A), phase (B) and elevation (C). Tidal elevation was processed using `ttide_py`¹ for tidal analysis and the `numpy` python library was used to calculate r-squared values.

¹ https://github.com/moflaher/ttide_py

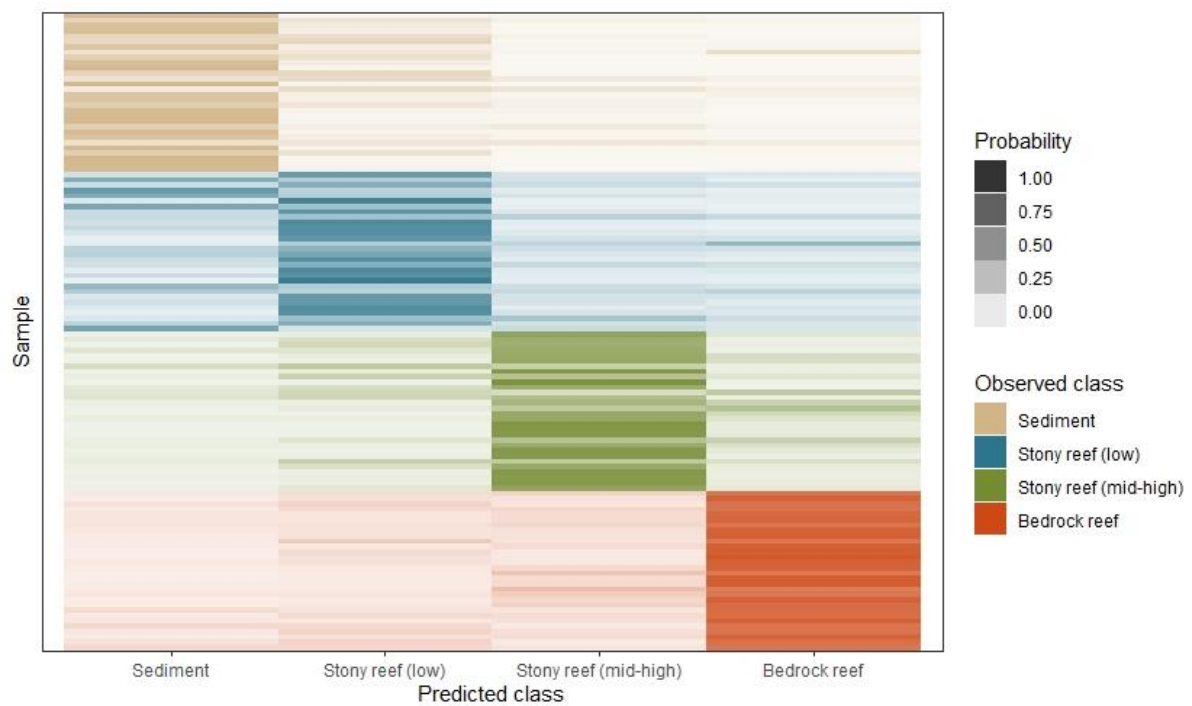


Figure S3. Heat map of predicted class probabilities for a random subset of samples (30 per observed class) from the reef substrate model.

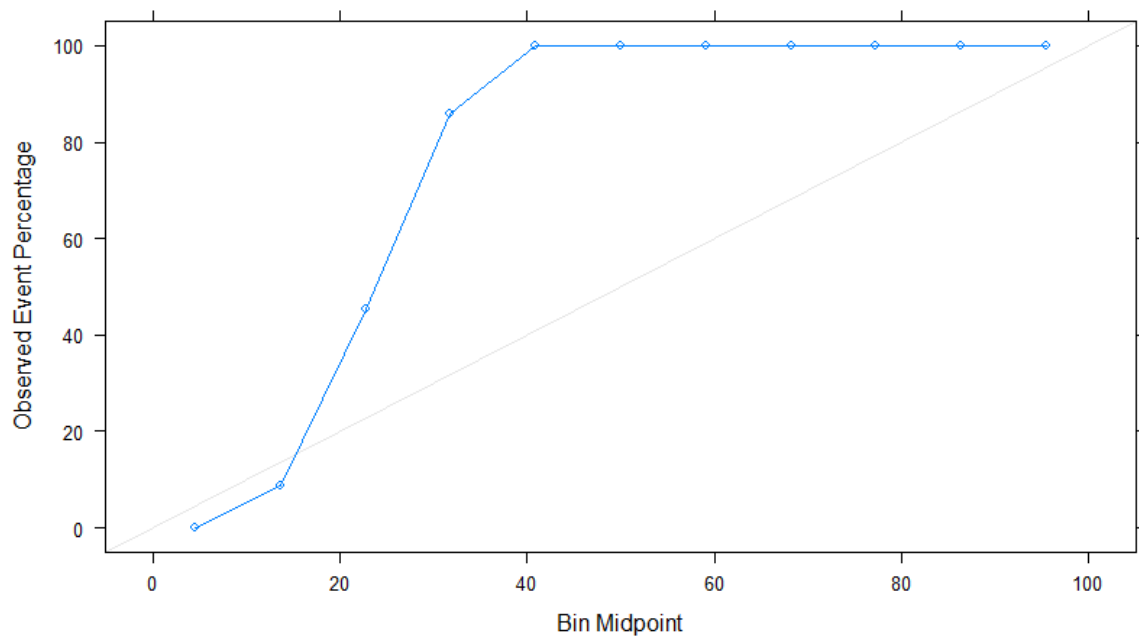


Figure S4. Reliability diagram for the *Sabellaria spinulosa* reef model. The model appears to underpredict *S. spinulosa* reef, treated as the event.